Journal of Nuclear Materials 386–388 (2009) 511–514

Contents lists available at ScienceDirect

Journal of Nuclear Materials

journal homepage: www.elsevier.com/locate/jnucmat

Evaluation of threshold stress of the MA957 ODS ferrtic alloy

H. Sakasegawa [a,*], L. Chaffron [b], F. Legendre [a], M. Brocq [a], L. Boulanger [a], S. Poissonnet [a], Y. de Carlan [b], J. Bechade [b], T. Cozzika [b], J. Malaplate [b]

[a] CEA Saclay, DEN/DANS/DMN/SRMP, 91191 Gif-sur-Yvette Cedex, France
[b] CEA Saclay, DEN/DANS/DMN/SRMA, 91191 Gif-sur-Yvette Cedex, France

A B S T R A C T

Threshold stress of ODS (Oxide Dispersion Strengthened) alloy is well known as a value which can quantitatively shows the effect of oxide dispersion strengthening. However, the threshold stress cannot be clearly observed in the result of creep tests for the commercial ODS alloy MA957. In this work, the threshold stress of MA957 was carefully evaluated using TEM (Transmission Electron Microscope) with EDS (Energy Dispersive X-ray Spectrometer). From the result, it was revealed that MA957 has an inhomogeneous dispersion of oxide particles. The inhomogeneous dispersion caused different threshold stresses between observed areas. This is probably a reason why the threshold stress cannot be clearly seen in the result of creep tests. This inhomogeneous dispersion appeared to be partly caused by aluminum contamination, because aluminum made much larger complex oxide particles than the fine oxide particles with no aluminum. Consequently, aluminum should be strictly controlled or eliminated for the homogeneous dispersion of oxide particles of MA957.

1. Introduction

ODS alloys are attractive structural materials for advanced fission and fusion reactors, because of their highly improved creep properties [1–8] and good irradiation resistance [3,9–16] compared to conventional ferritic/martensitic and austenitic steels. Such superior properties are obtained through nanosized oxide particles dispersed in the matrix. These nanosized oxides are very stable under heavy irradiation and at high temperatures. Consequently, many researches have been conducted to finely disperse oxide particles in the matrix by modifying chemical compositions and developing material processing procedures [17–22].

In general, creep properties of ODS alloys and creep mechanisms have been studied and analyzed using threshold stress and power law type equation. However, it is well known that threshold stresses cannot be clearly seen in results of creep tests and their stress exponent values are too high for any creep mechanisms theoretically explained [6,7,23].

In this work, the threshold stress of MA957 was carefully evaluated based on the result of TEM observation and the reason why the threshold stress cannot be clearly seen in creep tests was studied.

2. Experimental

The specimen used was the commercial ODS ferrtic alloy MA957 with a nominal composition of Fe–14Cr–0.3Mo–1.0Ti–0.25Y_2O_3 in wt%. A longitudinal section was cut from the specimen and ground to a thickness of about 100 μm for electropolishing. Punched discs with 3 mm diameter from the ground sheet were electropolished at 253 K using an electrolyte containing 10% perchloric acid in a mixture of ethyl alcohol with 20% butoxyethanol. The observation of oxide particles was performed using TEM with EDS. EPMA (Electron Probe X-ray Microanalyzer) was additionally used for observing micrometric structures.

3. Results and discussion

Fig. 1 gives a TEM image of grains in MA957. These grains were elongated parallel to the extrusion direction. Fig. 2 gives higher magnification TEM images with nanosized particles. In general, fine oxide particles can be only seen in areas with a very thin thickness around the hole of TEM disk. The thin area had locally bended parts, so imaging conditions locally changed. In this work, the observed areas were randomly selected keeping a long distance between them to obtain the information of nanosized particles from the entire sample. Fig. 3 gives the size distributions of oxide particles obtained from the image analysis results in Fig. 2. Differences of size distribution were seen between the observed areas. MA957 had an inhomogeneous dispersion of oxide particles.

* Corresponding author.
E-mail address: hideo.sakasegawa@cea.fr (H. Sakasegawa).

0022-3115/$ - see front matter © 2009 Elsevier B.V. All rights reserved.
doi:10.1016/j.jnucmat.2008.12.151

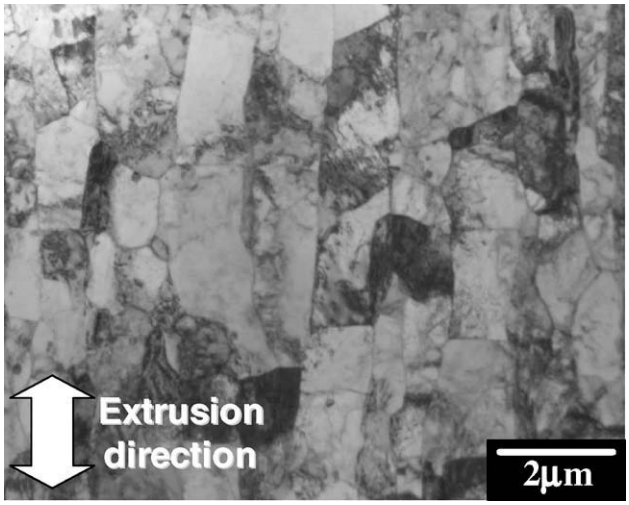

Fig. 1. TEM image of grains in MA957.

Chemical compositions of nanosized oxide particles were analyzed using EDS. The ratio of titanium to yttrium of the analyzed oxide particles are shown in Fig. 4 and the ratio was about 1. Therefore, these dispersed fine oxide particles were identified as $Y_2Ti_2O_7$.

Threshold stress can be calculated using the information of size distribution and the following equation [24,25] given by

$$\sigma_{th} = A\frac{MGb}{2\pi\bar{\lambda}}\left[\ln\left(\frac{\bar{D}}{r_0}\right) + B\right], \tag{1}$$

where A and B are constants which changes depending on strengthening mechanisms and characteristics of dislocation as shown in Table 1, M is the Taylor factor, G is the shear modulus, b is the Burgers vector, r_0 is the inner cut-off radius of dislocation core, $\bar{\lambda}$ is the average face to face distance between particles on a slip plane, and $\bar{D}$ is the harmonic mean of $2\bar{r}$ and $\bar{\lambda}$. $\bar{\lambda}$, $\bar{D}$, $\bar{l}_s$, and $\bar{\bar{r}}_s$ are calculated from the following equations:

$$\bar{\lambda} = 1.25\bar{l}_s - 2\bar{\bar{r}}_s, \tag{2}$$

$$\frac{1}{\bar{D}} = \frac{1}{2\bar{\bar{r}}_s} + \frac{1}{\bar{\lambda}}, \tag{3}$$

$$\bar{l}_s = \sqrt{\frac{2\pi}{3f}\frac{\overline{r^3}}{\bar{r}}}, \tag{4}$$

and

$$\bar{\bar{r}}_s = \frac{\pi}{4}\frac{\overline{r^2}}{\bar{r}}, \tag{5}$$

where r is the observed particle radius, and f is the volume fraction of the dispersed oxide particles. The volume fraction can be calculated using the contents of yttrium, titanium, and oxygen in MA957 and the density of the dispersed oxide. This was calculated under the assumption that all the oxide particles have the same phase as $Y_2Ti_2O_7$.

Fig. 5 shows the result of the calculation of threshold stress using the formulas (1) and the following values: $\nu = 0.34$, $G = 50\,600$ MPa, $M = 2$, $b = 0.248$ nm, $r_0 = b$ and $3b$ nm, $f = 0.6$ vol.% at 973 K. The temperature used is an expected operating temperature for ODS alloys. Calculated stresses have a range of about 100 MPa due to the difference of strengthening mechanism and the difference of the inner cut-off radius of dislocation core. It

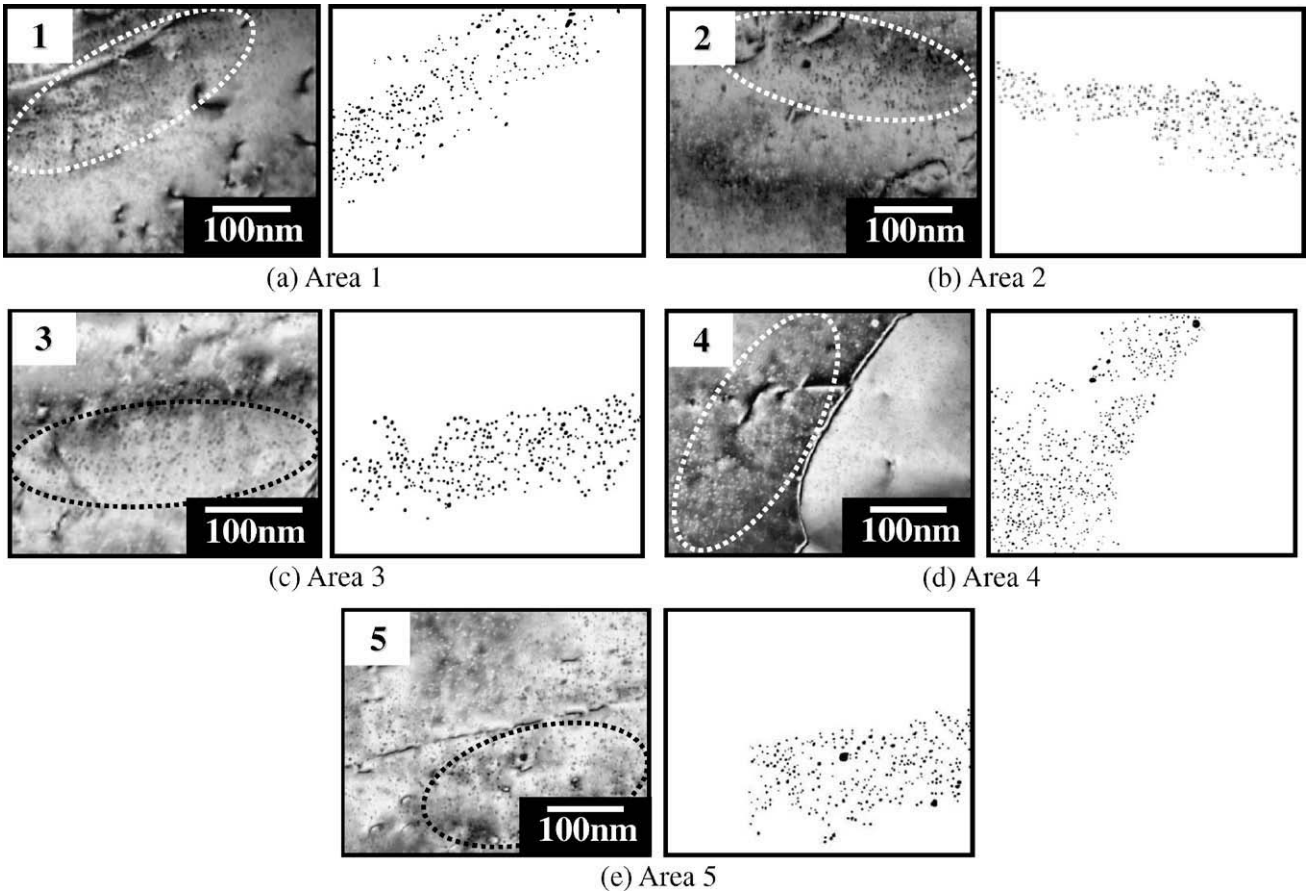

Fig. 2. TEM image of fine dispersed oxide particles and image analysis result.

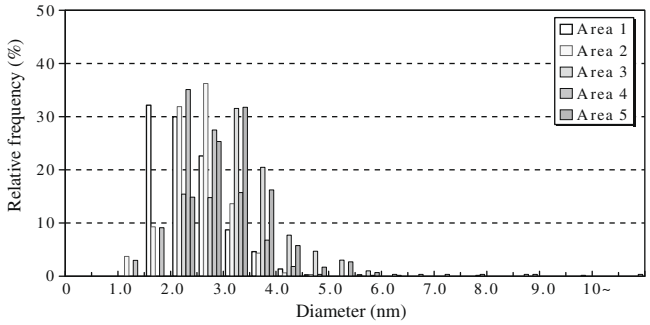

Fig. 3. Size distribution of fine dispersed oxide particles.

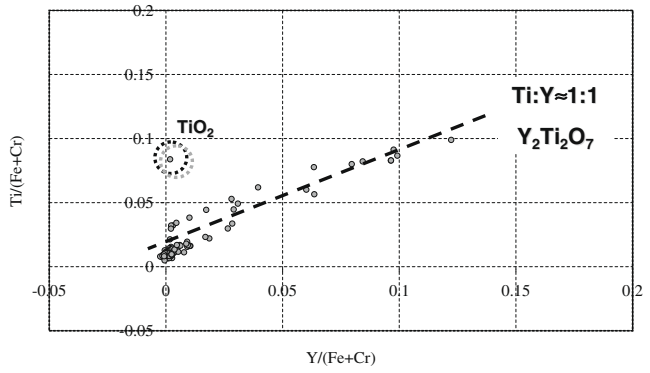

Fig. 4. Chemical composition map of Y–Ti–O oxide particles.

should be noted that two drops of threshold stress are evident at the area 3 and 5. The difference of size distribution affects the calculated threshold stresses and causes such a difference of up to 50 MPa. The threshold stress of MA957 varies between observed areas and a fixed value cannot be determined. This fluctuation of threshold due to the inhomogeneous dispersion probably causes localized creep deformation at high temperatures. This could be a reason why the threshold stress cannot be clearly observed in the result of creep tests.

The reason why MA957 had such an inhomogeneous dispersion has been studied. Fig. 6 shows the result of the observation using EPMA. Pores aligned in the extrusion direction were observed

Table 1
Parameter for the calculation of threshold stress.

Mechanism	Dislocation	A	B
Orowan	Edge	1	0.7
	Screw	$\frac{1}{1-\nu}$	0.6
Srolovitz	Edge	$\left(1-\frac{\nu}{1-\nu}\sin^2\phi\right)\cos\phi \quad \phi = 19^\circ$	0.7
	Screw	$\frac{1+\nu\sin^2\phi}{1-\nu}\cos\phi \quad \phi = 30^\circ + 48.3^\circ\nu$	0.6

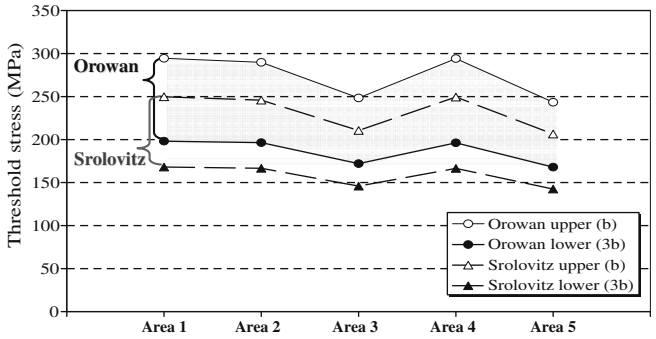

Fig. 5. Calculated threshold stress.

and aluminum was detected in them. The same structure was observed in other reports also [1,26]. Aluminum is not in the nominal composition of MA957. This is due to the contamination of powders. Coarse complex oxide particles containing aluminum were observed in the matrix as shown in Fig. 7. This complex oxide particle was probably composed of two oxides: Al–O and $Y_2Ti_2O_7$. Aluminum affected the formation of oxide particle and made a large oxide particle about 150 nm. Kasada et al. has studied ODS alloys with aluminum intended to improve corrosion resistance and reported the aluminum effect [27]. When ODS alloys contained aluminum, Y–Al–O oxides preferentially formed. These Y–Al–O oxide particles had larger sizes than Y–Ti–O oxides. The observed complex oxide particle was possibly a precursor based on his report. Further works are necessary for this. In the case of MA957, aluminum should be controlled and eliminated during the manufacturing process for the appropriate dispersion of oxide particles. It is very important to improve the homogeneity of dispersion for the reproducibility in mass production of ODS alloys in near future.

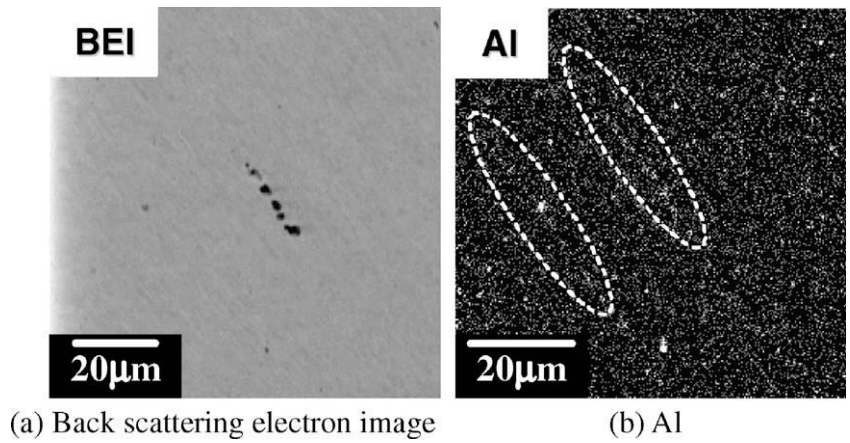

Fig. 6. Pores aligned in the extrusion direction.

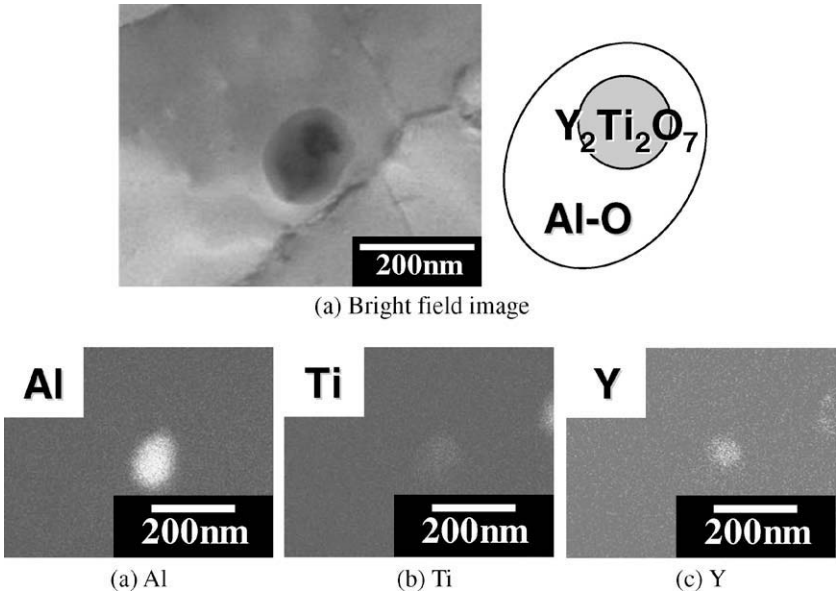

Fig. 7. Coarse complex oxide particle containing aluminum.

4. Summary

In this work, the threshold stress of MA957 was carefully evaluated and the reason why the threshold stress cannot be clearly observed in creep tests was studied. The results are summarized as follows:

- MA957 had an inhomogeneous distribution of oxide particles.
- Calculated threshold stresses varied between observed areas depending on different size distributions of oxide particles. This is probably a reason to explain the reason that the threshold stress cannot be clearly seen in creep tests.
- Aluminum, which is not in the nominal composition, was detected. This aluminum contamination affected formations of oxide particles. Aluminum contributed to form large complex oxide particles which were composed of Al–O and $Y_2Ti_2O_7$. Aluminum should be strictly controlled or eliminated for the homogeneous dispersion of oxide particles in MA957.

References

[1] R.L. Klueh, J.P. Shingledecker, R.W. Swindeman, D.T. Hoelzer, J. Nucl. Mater. 341 (2005) 103.
[2] R. Lindau, A. Möslang, M. Rieth, M. Klimiankou, E. Materna-Morris, A. Alamo, A.-A.F. Tavassoli, C. Cayron, A.-M. Lancha, P. Fernandez, N. Baluc, R. Schäublin, E. Diegele, G. Filacchioni, J.W. Rensman, B.v.d. Schaaf, E. Lucon, W. Dietz, Fus. Eng. Technol. 75–79 (2005) 989.
[3] M.B. Toloczko, D.S. Gelles, F.A. Garner, R.J. Kurtz, K. Abe, J. Nucl. Mater. 329–333 (2004) 352.
[4] A. Alamo, V. Lambard, X. Averty, M.H. Mathon, J. Nucl. Mater. 329–333 (2004) 333.
[5] S. Ukai, T. Kaito, S. Ohtsuka, T. Narita, M. Fujiwara, T. Kobayashi, ISIJ Int. 43 (2003) 2038.
[6] S. Ukai, S. Mizuta, M. Fujiwara, T. Okuda, T. Kobayashi, J. Nucl. Sci. Technol. 39 (2002) 778.
[7] S. Ukai, T. Okuda, M. Fujiwara, T. Kobayashi, S. Mizuta, H. Nakashima, J. Nucl. Sci. Technol. 39 (2002) 872.
[8] S. Ukai, M. Fujiwara, J. Nucl. Mater. 307–311 (2002) 749.
[9] H. Kishimoto, K. Yutani, R. Kasada, O. Hashitomi, A. Kimura, J. Nucl. Mater. 367–370 (2007) 179.
[10] K. Yutani, H. Kishimoto, R. Kasada, A. Kimura, J. Nucl. Mater. 367–370 (2007) 423.
[11] S. Yamashita, N. Akasaka, S. Ukai, S. Ohnuki, J. Nucl. Mater. 367–370 (2007) 202.
[12] R. Schäublin, A. Ramar, N. Baluc, V. de Castro, M.A. Monge, T. Leguey, N. Schmid, C. Bonjour, J. Nucl. Mater. 351 (2006) 247.
[13] T. Yoshitake, Y. Abe, N. Akasaka, S. Ohtsuka, S. Ukai, A. Kimura, J. Nucl. Mater. 329–333 (2004) 342.
[14] S. Yamashita, N. Akasaka, S. Ohnuki, J. Nucl. Mater. 329–333 (2004) 377.
[15] N. Akasaka, S. Yamashita, T. Yoshitake, S. Ukai, A. Kimura, J. Nucl. Mater. 329–333 (2004) 1053.
[16] I.-S. Kim, J.D. Hunn, N. Hashimoto, D.L. Larson, P.J. Maziasz, K. Miyahara, E.H. Lee, J. Nucl. Mater. 280 (2000) 264.
[17] S. Ohtsuka, S. Ukai, H. Sakasegawa, M. Fujiwara, T. Kaito, T. Narita, J. Nucl. Mater. 367–370 (2007) 160.
[18] H. Sakasegawa, S. Ohtsuka, S. Ukai, H. Tanigawa, M. Fujiwara, H. Ogiwara, A. Kohyama, J. Nucl. Mater. 367–370 (2007) 185.
[19] S. Ohtsuka, S. Ukai, M. Fujiwara, T. Kaito, T. Narita, J. Phys. Chem. Solids 66 (2005) 571.
[20] S. Ohtsuka, S. Ukai, M. Fujiwara, T. Kaito, T. Narita, Mater. Trans. 46 (2005) 487.
[21] S. Ohtsuka, S. Ukai, M. Fujiwara, T. Kaito, T. Narita, J. Nucl. Mater. 329–333 (2004) 372.
[22] H. Sakasegawa, M. Tamura, S. Ohtsuka, S. Ukai, H. Tanigawa, A. Kohyama, M. Fujiwara, J. Alloys Compd. 452 (2008) 2.
[23] H. Sakasegawa, S. Ukai, M. Tamura, S. Ohtsuka, H. Tanigawa, H. Ogiwara, A. Kohyama, M. Fujiwara, J. Nucl. Mater. 373 (2008) 82.
[24] J.W. Martin, Micromechanisms in Particle-Hardened Alloys, Cambridge University, 1980.
[25] A.J.E. Foremann, M.J. Makin, Philos. Mag. A14 (1966) 911.
[26] M.J. Alinger, G.R. Odette, G.E. Lucas, J. Nucle. Mater. 307–311 (2002) 484.
[27] R. Kasada, N. Toda, K. Yutani, H.S. Cho, H. Kishimoto, A. Kimura, J. Nucl. Mater. 367–370 (2007) 222.